Eleventh South African Conference on Computational and Applied Mechanics
SACAM 2018
Vanderbijlpark, South Africa, 17-19 September 2018

Estimation of probability of defect detection by combining simulated defect signatures with measured ultrasonic guided wave signals

Dineo A. Ramatlo[a,b], Philip W. Loveday[b], Craig S. Long[b], Daniel N. Wilke[a]

[a]*University of Pretoria, Private Bag X20, Hatfield 0028, Pretoria, South Africa*

[b]*CSIR, PO Box 395, Brummeria 0001, Pretoria, South Africa*

Email address: DRamatlo@csir.co.za[a], PLoveday@csir.co.za[b], CLong@csir.co.za[c], nico.wilke@up.ac.za[d]

Abstract

Continuously welded heavy haul railway lines experience very large stresses due to high axle loads and varying environmental conditions. These extreme loading conditions can lead to the development of cracks and eventually rail breaks, which are the most common cause of train derailment. The need to detect rail breaks led to development of the Ultrasonic Broken Rail Detection (UBRD) System, making it possible to detect only complete rail breaks. Current research efforts are aimed at detecting damage such as cracks before a complete break occurs, at long range using guided wave ultrasound. A method to quantify the probability of detecting various damage types would be very useful to evaluate system performance during the development phase. Cracks growing in rails can be detected by comparing numerous ultrasonic signals, recorded using a permanently installed monitoring system, over a period of time. These signals will contain reflections from benign structural features (such as welds) which do not represent damage, as well as potentially small but growing reflections from damage. Variations in environmental and operational conditions may produce large changes in the ultrasonic signals thereby masking the damage. The challenge is therefore to distinguish between these benign signals and the true damage signals. This task is further complicated by the fact that obtaining monitoring data for different damage scenarios under varying environmental and operational conditions is virtually impossible since detected defects in sections of an operational rail track are immediately removed and replaced with new rail. Laboratory damage experiments are also not possible due to end reflections from short sections of rail dominating the response. Therefore, damage signals can only practically be obtained from numerical simulations. The aim of this paper is to demonstrate a procedure to combine simulated damage signals and measured data obtained under operational conditions, concentrating specifically on temperature variations. Unsupervised machine leaning algorithms for extracting and classifying signal features associated with different sources from measurements are then be applied to detect and classify the synthetic damage. Receiver Operator Characteristic curves, which plot the probability of detection against the probability of false alarm, are then estimated for selected damage scenarios.

Keywords: Probability of Damage Detection, Environmental and Operational Conditions, Receiver Operator Characteristic Curves, Guided Wave Ultrasound

1. Introduction

The development of a reliable monitoring system for defect detection in rails is still of great significance to the rail industry as it guarantees a solution to the problem of train derailments caused by broken rails. An example of a currently existing system which was developed to fulfil such a purpose is the Ultrasonic Broken Rail Detection System (UBRD). The system detects complete breaks in railway lines by relying on ultrasonic guided waves propagating the head of the rail, transmitted from and received by piezoelectric transducers, [1]. Since April 2016, the installation of the UBRD system on the Sishen-Saldanha Ore line has reported seven rail breaks and a number of major flaws [2] which were recorded as false alarms as the system was designed to detect only complete breaks. Detecting complete rail breaks and halting train operation generally prevents derailments. Rail breaks can occur under a train and in this case can cause derailment of part of the train. Detecting a crack before the rail breaks would avoid these derailments and also allow condition based maintenance. Current research efforts are aimed at upgrading the UBRD system to include this functionality while relying on multiple propagating modes to achieve complete coverage of the rail cross-section. The employment of multiple ultrasonic guided wave modes would allow for damage detection anywhere in the rail, Fig 1.

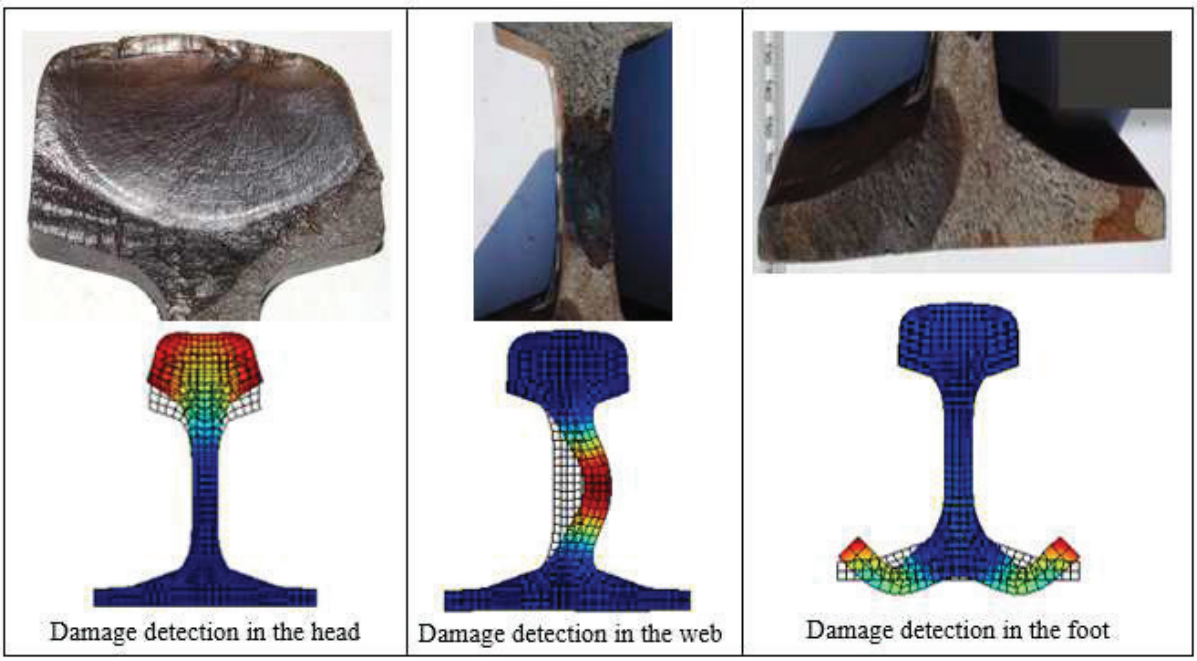

Fig. 1. Guided wave modes for detecting damage in different regions of the rail

Damage in rails can be detected from ultrasonic signals containing reflections from different structural features where some of the reflections would be due to any damage present in the rail. The procedure would be to collect measured signals from a rail track for a specified time frame over which damage is growing; and then employ appropriate algorithms to distinguish and classify the reflections according to their sources; and thereafter determine and locate the reflection coming from damage. Liu et.al [3] demonstrated the application of this procedure to pipelines where unsupervised machine learning algorithms were adopted to detect corrosion. Although superficially, application of this proposed technique to pipe and rail problems may appear similar, there are important differences which present challenges in rail applications. Specifically in our application, many more modes are excited and propagation is generally dispersive in our case, making signal processing significantly more challenging. Furthermore, variations in environmental (e.g. temperature) and operational (e.g. passing trains) conditions may produce large changes in the ultrasonic signals thereby masking the damage. The challenge is therefore to distinguish between these benign signals and the true damage signals. One major challenge which we would like to address in this paper is that of obtaining ultrasonic data containing damage signatures. For both pipelines and rail tracks, obtaining monitoring data for different damage scenarios under varying environmental and operational conditions is virtually impossible since detected defects in sections of an operational waveguide are immediately removed and replaced. The alternative has thus been to carry out a series of laboratory experiments while inducing a growing damage on the waveguide test piece. However, laboratory damage experiments are also not possible for rail tracks due to end reflections from short sections of rail

dominating the response. Therefore, damage signals for rails can only practically be obtained from numerical simulations.

The aim of this paper is to demonstrate a procedure to combine simulated damage signals and measured data obtained under operational conditions, concentrating specifically on temperature variations. A method to quantify the probability of detecting various damage types would be very useful to evaluate system performance during the development phase. We thus further extend the study to quantify the performance of damage detection schemes by estimating the probabilities of detection and false alarms.

Firstly, field measurements from a damage-free rail subjected to real operational conditions are obtained. Thereafter artificial damage signals computed using numerical simulations, and modified to represent the appropriate operational conditions, are added to the experimental signals. To this point, the three damage detection schemes which have been identified and proven to be effective when applied to GWU are Baseline Subtraction, Independent Component Analysis and Singular Value Decomposition [4]. In this paper we only explore the baseline subtraction and ICA methods when applied to a synthetic dataset (field measurements combined with simulated damage) respectively, to classify and detect the imposed damage. Using Receiver Operator Characteristic (ROC) curves, the probabilities of detection are determined for the selected damage scenario. In future studies, ROC curves will be used to improve the reliability of the system by minimizing false alarms and optimizing true detections.

Guided waves are complex in nature due to their multi-modal and dispersive nature. To account for this, several pre-processing techniques are employed to simplify the recorded signals. Dispersion causes a pulse of energy to spread out in space and time as it propagates. A dispersion compensation procedure [5] which maps measurements from the time domain to distance domain, is thus carried out with the purpose of removing the dispersion effects from guided wave signals. In the mapping process, dispersed signals are compressed to their original shape. To account for variations brought by temperature change, the measurements are brought to the same baseline by applying a temperature compensation strategy proposed by Harley et.al [6]. Thus far, other operational and environmental conditions (EOCs) affecting field measurements are not yet known and thus still needs to be determined and compensated for.

The procedure steps followed to detect damage and quantify the probabilities of detection are summarized in Fig 2.

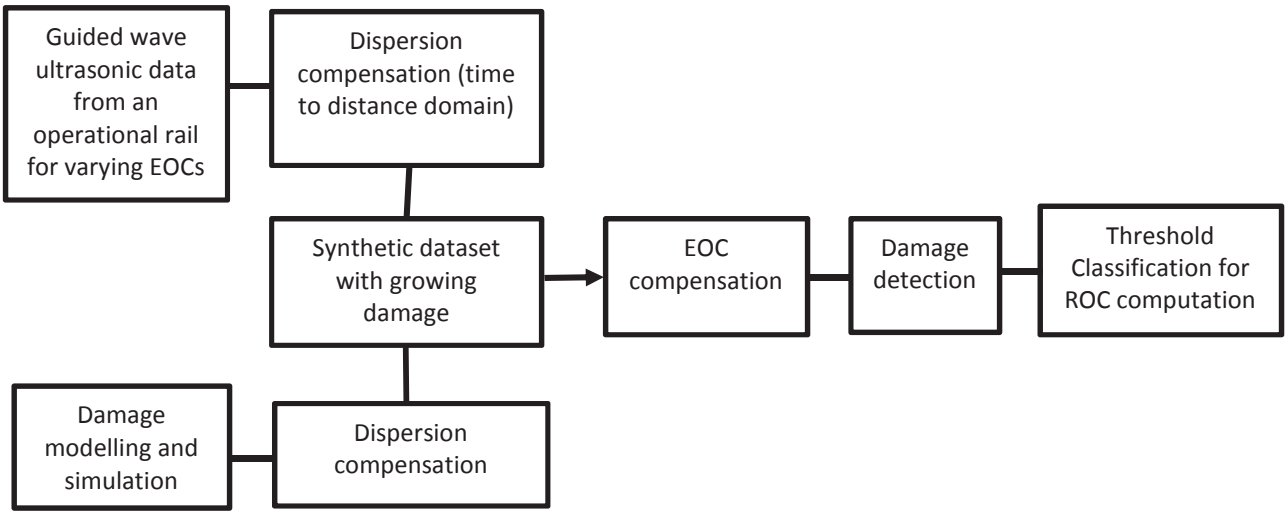

Fig. 2. The procedure steps employed to detect damage and quantify the probabilities of detection

2. Problem Description

Consider a schematic representation of an operational railway line plotted in Fig 3. The track is made up of an effectively infinite number of $240m$ long sections, joined with aluminothermic welds. Suppose that just after weld C, there exist a growing defect (i.e. a crack) within the rail, which we would like to detect and quantify its probability of detection.

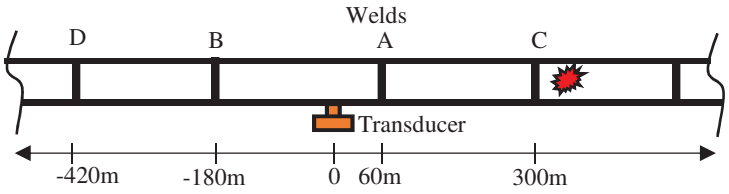

Fig. 3. Schematic representation of an operational railway line with damage just after weld C

The rail track is exposed to real operational (passing trains and external noise) and environmental (i.e. temperature variations) conditions. The ultrasonic data measured from the rail will therefore be influenced by these conditions.

3. Synthetic dataset with growing damage

To be able to detect the damage in the rail using machine learning algorithms, we need to collect a set of similar measurements over a specified period of time during which damage progression is monitored. To solve the hypothetical problem in Section 2, we employ the procedure in Fig 2 to superimpose simulated defect signals on measured data from an operational rail, to generate the synthetic dataset.

A dataset of 50 guided wave reflection signals under different environmental and operational conditions were collected from a damage free operational rail way line using a piezoelectric transducer attached to the rail. It is assumed that during the time frame over which these signals are collected, a damage would initiate and grow in the rail. The guided waves in the rail were excited using a transmitting transducer driven using a 17.5 Hanning windowed tone burst voltage signal at a center frequency of 35kHz. The same transducer was also used as a sensor to receive the reflections. Fig 4a below shows two measurement signals collected at different temperature readings. In Fig 4b, the signals are mapped to the distance domain using Wilcox's dispersion compensation procedure [5] combined with a simple filtering procedure to remove unwanted frequencies from the signals. The wave packet envelope is plotted in Fig 4b. The reflections from the welds are clearly visible in the distance domain.

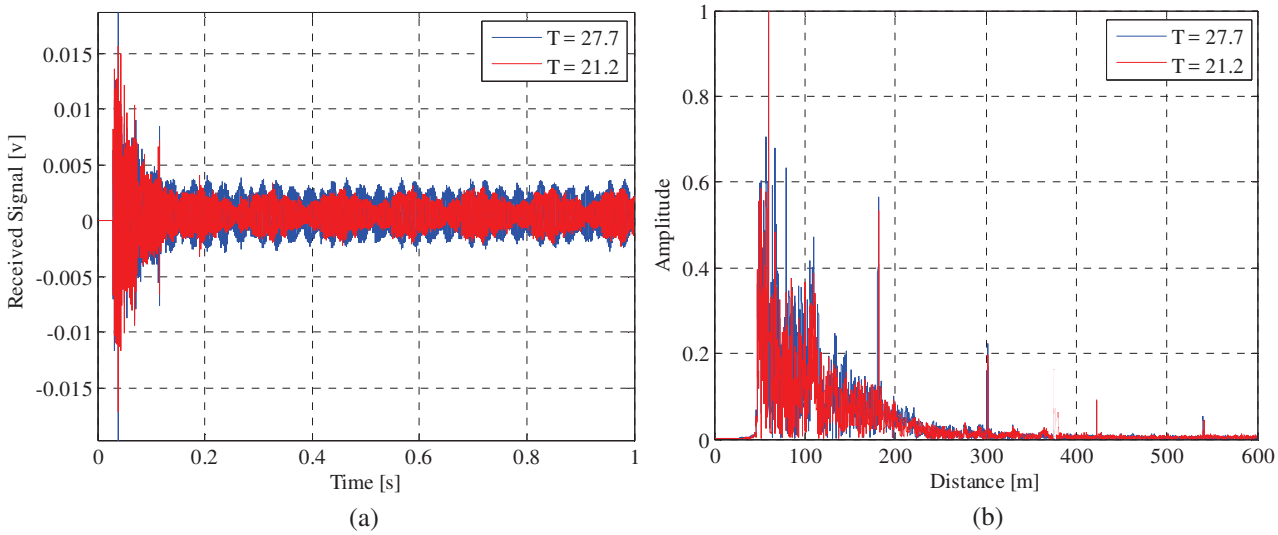

Fig. 4. Field measurement signals at two temperature conditions in the (a) time domain and (b) distance domain after dispersion compensation

For each of the 50 collected measurements, a number of 50 growing damage signals were respectively superimposed to generate a synthetic dataset for a linear growth pattern damage progression scenario. Simple damage signals were simulated by simply propagating a 17.5 Hanning windowed tone burst signal at a center frequency of 35kHz to the appropriate location distance. The modelling technique proposed by [7], which combines the traditional 3D finite element procedure [8] for modelling the near field surrounding the damage and the Semi-Analytical Finite Element (SAFE) method [9], [10] for modelling the ingoing and outgoing waves from the damage region is still under evaluation and will be adopted in future to achieve realistic damage models. A displacement field equation adopted from the Semi-Analytical Finite Element method [9] for modelling ultrasonic wave propagation was used to produce damage signals in the time domain:

$$y(t) = y_0(t)\mathrm{e}^{-\mathrm{i}(\mathrm{k}(\omega)\mathrm{z}-\omega\mathrm{t})} \tag{1}$$

where y_0 is the tone burst signal, t is the time, ω is the frequency, k is the wavenumber of the propagated mode computed from a SAFE model of the rail and z is the distance through which the wave is propagated.

EOC conditions such as temperature will have a random variation for the measurements in the dataset while damage size will grow from the measurement collected at the earliest time to the last measurement collected. When a waveguide in which an ultrasonic signal propagates, is subjected to a temperature change, the time of arrivals for the reflections will change. A temperature increase will cause the reflections to arrive late in time. This is because temperature change slightly changes the Young's Modulus of the rail. The Young's Modulus of the rail is related to temperature through:

$$E = E_0 - \frac{\partial E}{\partial T}(T - T_0) \tag{2}$$

where E_0 and T_0 are respectively the Young's Modulus and temperature of the baseline distance of propagation. A change in the Young's Modulus causes a change in the group velocity of the wave in the rail. If this change is not included in the dispersion compensation procedure the distance to a reflector will appear to change with temperature. The apparent propagation distance for a specified temperature reading was evaluated as:

$$z = (1 + 0.00013T)z_0 \tag{3}$$

z_0 is the baseline propagation distance. Equation 3 was deduced after evaluating the influence of temperature on field measurements. The damage signatures were thus added at the correct location by including temperature effects in the model using equations 2, 3 and 1. Other EOCs which are not yet known at this point, are still to be investigated. The inclusion of damage to field measurements was carried out in the distance domain after performing dispersion compensation.

Figures 5a and 5b shows the temperature history and damage locations for each measurement in the dataset, respectively. In Fig 5c and Fig 5d the first, $26th$ and last measured signals are plotted, with measurement 1 having no damage and measurement 50 having the maximum damage with an amplitude of 0.35. This maximum damage is small compared to cracks that have led to broken rails and was selected to compare the capabilities of different detection methods.

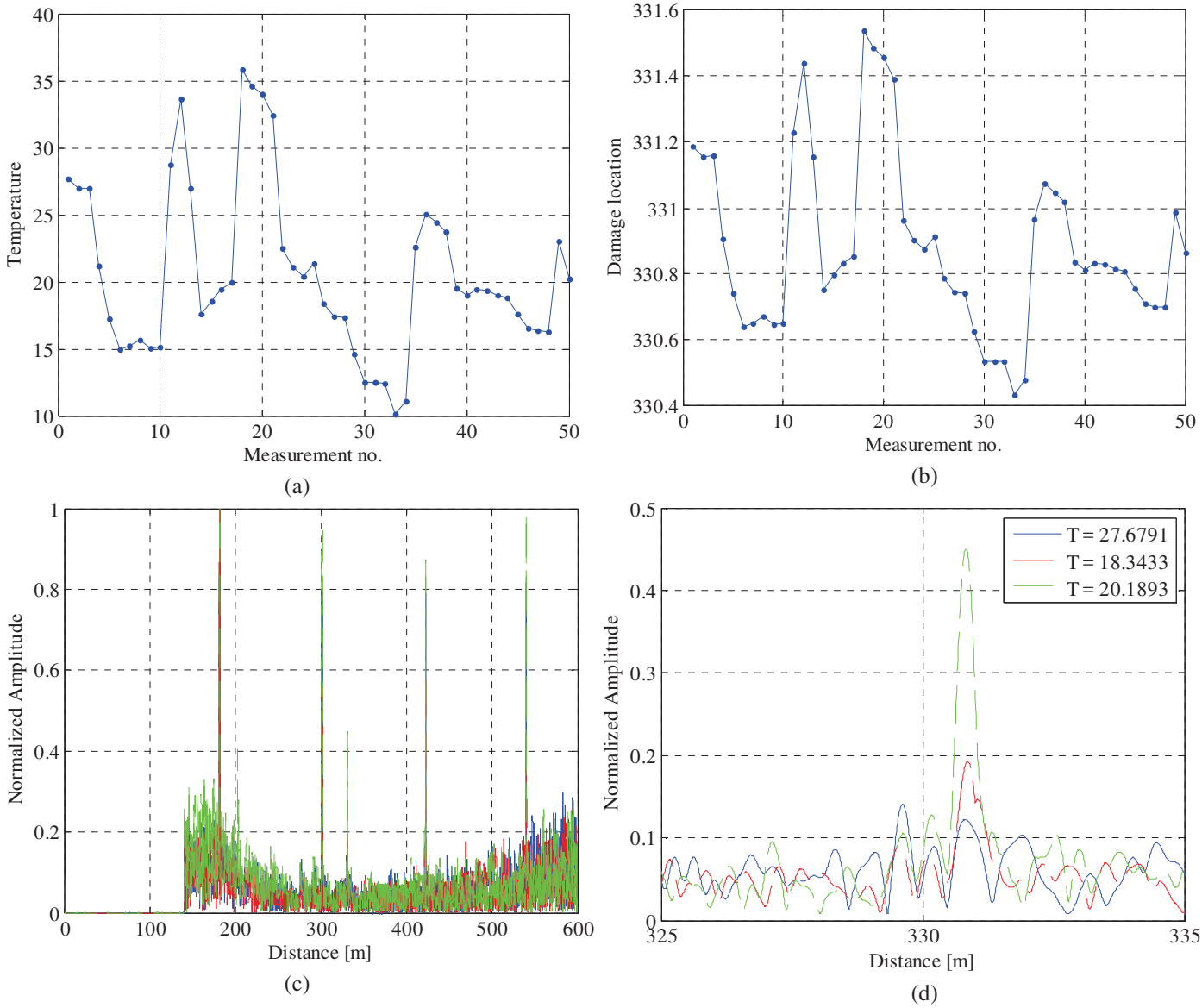

Fig. 5. (a) The temperature history and (b) damage locations for a dataset of 50 signals with (c) & (d) a plot of the first, 26th and last signals in the dataset

As the synthetic dataset was generated for different practical EOCs, it is significant to compensate for this EOC difference before any further processing. This will help to improve the performance of the damage detection technique used. EOC compensation will help to bring the measurements to the same baseline by aligning the reflections such that when the residuals are evaluated, only the components associated with damage will remain. Thus far, the known EOCs affecting guided waves in rails are noise from a moving train, stochastic noise and temperature. Other EOCs are not yet known and proven to exist. Noise from a moving train was compensated for during the data collection stage by avoiding taking measurements when a train was passing. Stochastic noise was accounted for by filtering out unwanted frequencies from the signals and temperature was compensated for using the method proposed by [6].

4. Damage Detection

To identify damage signatures from the synthetic data, we employ the baseline subtraction and ICA methods. In the Conventional Baseline Subtraction (CBS) method, *50* residual signals are computed by subtracting the first collected measurement (the baseline signal without damage) in the dataset from subsequent measurements with growing damage. Thereafter, we fit *m* (where m is the number of discrete distance points in the signals) linear regression models to these residual signals at each distance point x using the least squares equation, where the intercepts (β_{x0}) and slopes (β_{x1}) are determined from equation 4.

$$r_{xi} = \beta_{x0} + \beta_{x1} t_i + e_i \tag{4}$$

The β_{x1} values are then used to identify the growing damage contained in the measurement signals. Detail explanations of this method are included in [3].

In the ICA method explained in [11], damage is detected using blind source separation where the unknown source signals (independent components - ICs) are determined from the synthetic dataset using independent component analysis where a principal component analysis method is first employed. It is expected that damage should be extracted as one of the independent components. We detect damage by determining the independent component associated with an increasing weighting factor.

5. Receiver Operator Characteristic Curves

After the damage identification process is complete, the performance of the detection technique is quantified using ROC curves.

To compute ROC, we first identify the correct damage region as explained above for CBS and ICA, respectively. Then we classify all the points in the correct damage region as the Total True Positives (*TTPs*). All the other points in the signal are classified as the Total False Positives (*TFPs*). The next step is then threshold classification, where we sweep a threshold line from zero to one on a normalised residual signal (or independent component signal for ICA). For every threshold value, all the points above the threshold that falls within the true damage region are classified as the True Positives (*TPs*) and the rest of the points above the threshold line but not within the true damage region are classified as the False Positives (*FPs*). Then a point on the ROC curve is associated with each threshold value and evaluated from equations 5 and 6. Fig 6 below illustrates the computation of a ROC curve.

$$Probability\ of\ false\ alarm\ (FPR) = \frac{FP}{TFP} \tag{5}$$

$$Probability\ of\ detection\ (TPR) = \frac{TP}{TTP} \tag{6}$$

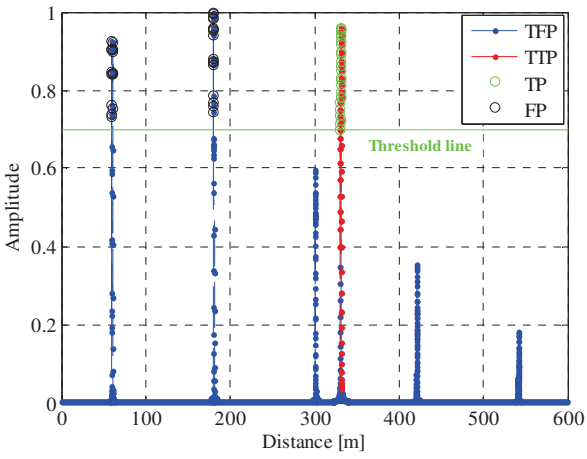

Fig. 6. An illustration for ROC curve computation

6. Results

6.1. Baseline Subtraction

In Figs 7a-c, the residuals obtained from baseline subtraction, linear regression models (equation 4) and the slope (β_{x1} from equation 4) are plotted, respectively. The reflection associated with damage was identified using the β_{x1} coefficient. It is evident from the results that the temperature compensation strategy did not yield good results for measured data. With perfect compensation, it is expected that that residual signals will have approximately zero amplitude everywhere else except at the damage location. The residual signals still contain non-damage related components. This is a clear indication that temperature is not the only EOC present in the measurements hence the temperature compensation strategy did not successfully bring the signals to the same baseline, with damage growth being the only difference.

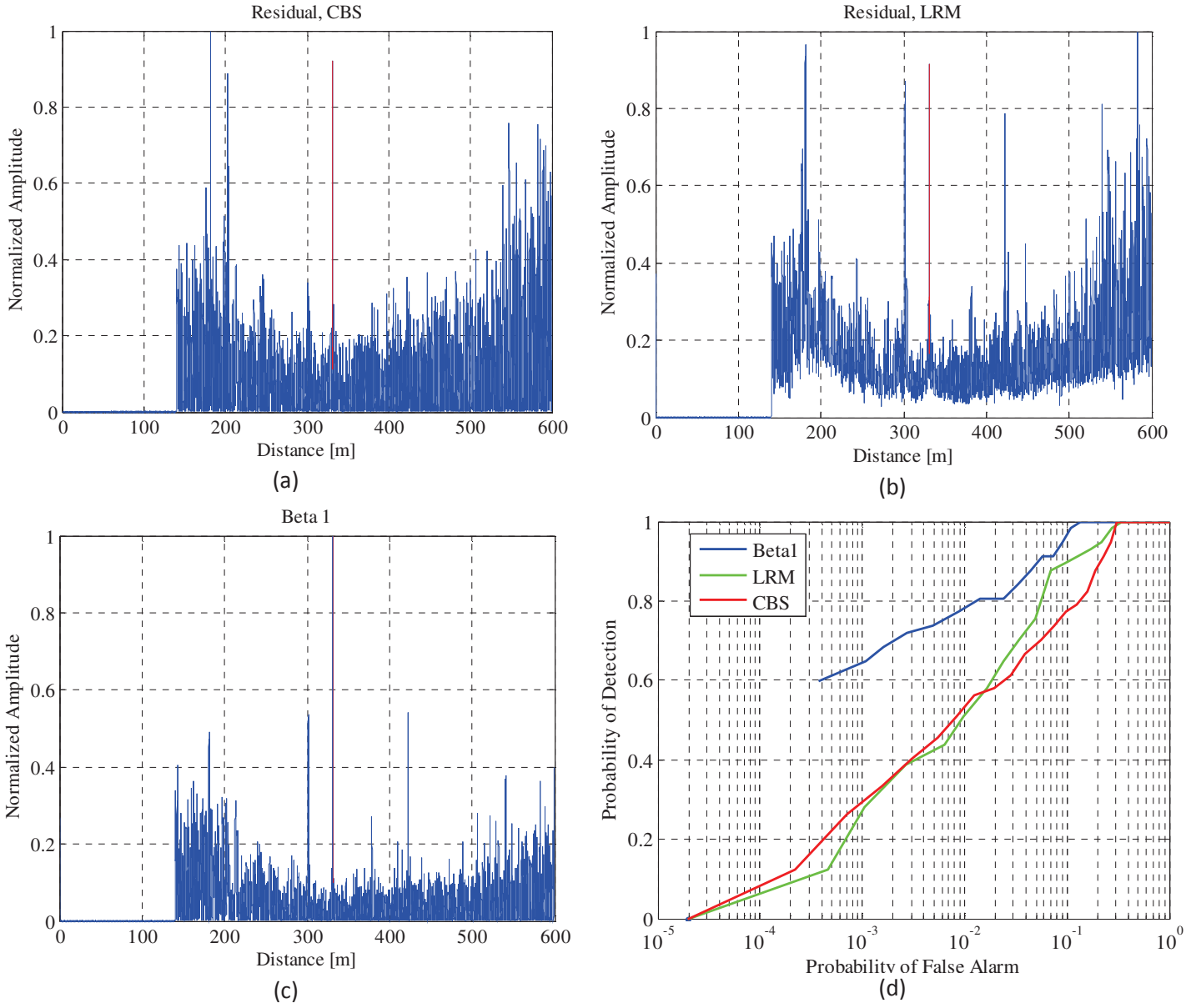

Fig. 7. (a) Baseline subtraction and (b) linear regression residuals with (c) the obtained $\boldsymbol{\beta_{x1}}$ values and their associated (d) ROC curves for measured data fused with simulated damage (with temperature compensation)

The ROC curves evaluated using the signals in Figs 7a-c are superimposed on the same plot in Fig 7d. The ROC curves shows that the damage signatures could be detected though there is a possibility of a false alarm. When the threshold is above the damage region, no damage will be detected. Fig 6d shows that the β_{x1} coefficient has a better performance. It is expected that after compensating for all the EOCs present, the performance level will improve drastically as the residual signals will mainly contain the damage reflection.

6.2. ICA

Using the ICA method, the principal components (PCs), independent components (ICs) and their associated weighting factors were evaluated. The weighting factors were used to identify the components related to damage with the expectation that it should have an increasing or decreasing trend.

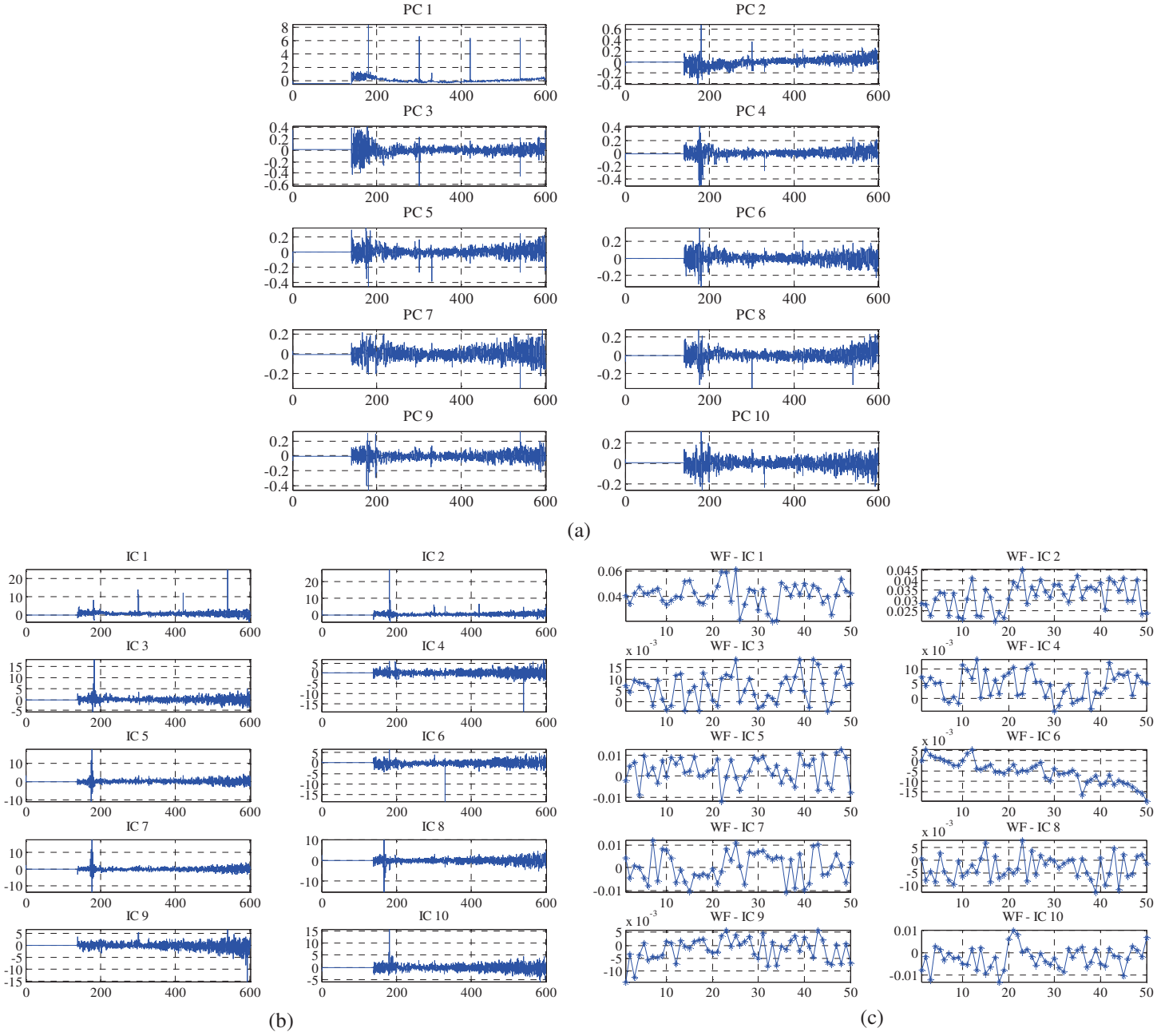

Fig. 8. Field data fused with growing damage with temperature compensation, (a) principal components, (b) independent components and their (c) weighting factors (WF)

In Fig 8, the results from ICA are plotted, showing only the first ten components from the 50 which were computed. Principal component analysis is the first step to signal separation. In Fig 8a, the weld components can be clearly seen in PC 1, the damage component appears in PCs 5 and 10 while noise is present in almost all the components. In Fig 8b, we see that a further separation of the reflections according to their sources was performed. The weighting factors in Fig 8c shows a random variation with WF 6 showing a global increasing trend, indicating that IC 6 in Fig 8b is the damage component.

The ROC curve for IC 6 is plotted in Fig 9 below. It is seen that the performance here is better than that obtained for baseline subtraction method.

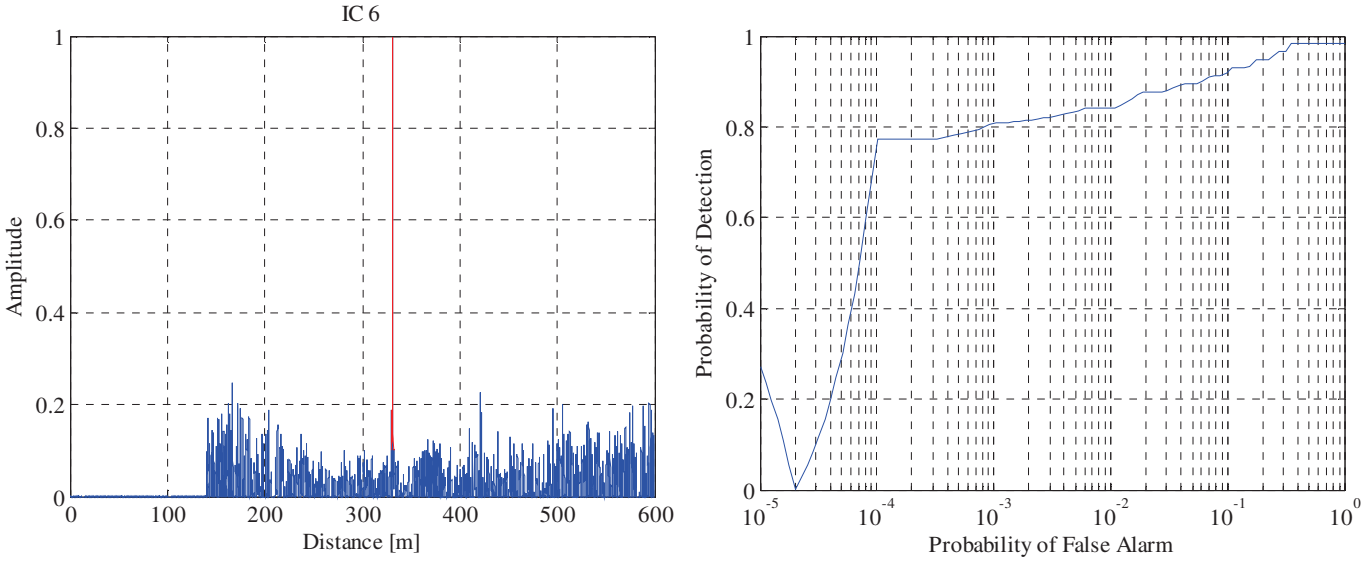

(a) (a)

Fig. 9. (a) The damage component IC 6, and (b) the associated ROC performance

7. Conclusion and future work

The aim of this paper was to demonstrate a procedure to combine simulated damage signals and measured data obtained under operational conditions; detect the damage signatures, and thereafter quantify the performance of the damage detection schemes by estimating the probabilities of detection and false alarms. Simulated damage signals and experimental field signals were combined using superposition. Damage was detected using a baseline subtraction method and an ICA method, respectively. The performance of damage detection was quantified using ROC curves. It was found that the ICA method performed better than the baseline subtraction method.

Although temperature was the only EOC considered, it was evident from the results that other EOCs are also present and are highly influencing the guided wave signals. This led to the performance of the damage detection techniques being bad and indicating high probabilities of false alarms.
It is expected that if we can compensate for all the EOCs present, the damage detection schemes (baseline subtraction and ICA) will be able to detect damage with a higher probability of detection and less false alarms. Other EOCs thus needs to be identified and properly compensated for.

This paper has successfully demonstrated a framework for designing monitoring systems to detect damage in rails. In future work, the framework will be improved by considering the following:

- Using the method of Benmeddour [7] to model realistic damage signals.
- Identify other EOCs affecting the monitoring data and establish ways to compensate for them.
- Adopt non-linear ICA methods for damage detection. It is expected that non-linear ICA will compensate for the non-linearities brought by EOC variations.

References

[1] Burger FA, Loveday PW, Long CS (2015). *Large Scale Implementation of Guided Wave Based Broken Rail Monitoring*, 41st Annual Review of Progress in Quantitative Nondestructive Evaluation, 771–776.

[2] Burger FA, Loveday P (2017). *Ultrasonic broken rail detector and rail condition monitor technology.* In Proceedings of the 11th International Heavy Haul Association Conference (IHHA 2017), Cape Town, South Africa, 275–280.

[3] Liu C, Dobson J, Cawley P (2017). *Efficient generation of receiver operating characteristics for the evaluation of damage detection in practical structural health monitoring applications*. Proceedings Royal Society, **437**: 1–26.

[4] Liu C, Dobson J, Cawley P (2016). *Practical Ultrasonic Damage Monitoring on Pipelines Using Component Analysis Methods,* 19th World Conference on Non-Destructive Testing, 1–8.

[5] Wilcox PD (2003). *A Rapid Signal Processing Technique to Remove the Effect of Dispersion from Guided Wave Signals*. IEEE Transactions on Ultrasonics, Ferroelectrics, and Frequency Control, **50(4)**: 419–427.

[6] Harley JB, Moura JMF (2012). *Scale Transform Signal Processing for Optimal Ultrasonic Temperature Compensation*. IEEE Transactions on Ultrasonics, Ferroelectrics, and Frequency Control, **59(10)**: 2226–2236.

[7] Benmeddour F, Treyssède F, Laguerre L (2011). *Numerical modeling of guided wave interaction with non-axisymmetric cracks in elastic cylinders.* International Journal of Solids and Structures, **48(5)**: 764–774.

[8] Cook RD (1995). *Finite Element Modeling For Stress Analysis*. John Wiley & Sons, Inc.

[9] Hayashi T, Song WJ, Rose JL (2003). *Guided wave dispersion curves for a bar with an arbitrary cross-section, a rod and rail example.* Ultrasonics, **41(3)**: 175–183.

[10] Gavric L (1995). *Computation of Propagative Waves in Free Rail Using a Finite Element Technique*. Journal of Sound and Vibration, **185**: 531–543.

[11] Hyvärinen A, Oja E (2000). *Independent Component Analysis : Algorithms and Applications*. Neaural Networks, **13**: 411–430.